Structure of Dierbium Decavanadate 25-Hydrate, $Er_2V_{10}O_{28}.25H_2O$

By B. E. Rivero,* G. Rigotti* and G. Punte†

Departamento de Física, Facultad de Ciencias Exactas, UNLP, CC 67, La Plata 1900, Argentina

and A. Navaza

Faculté de Pharmacie, 92 Châtenay-Malabry, France

Abstract. $M_r = 1741.52$, triclinic, $P\bar{1}$, $a = 9.168$ (9), $b = 10.002$ (15), $c = 12.703$ (6) Å, $\alpha = 68.87$ (8), $\beta = 77.52$ (8), $\gamma = 89.34$ (10)°, $V = 1058$ Å^3, $Z = 1$, $D_m = 2.66$, $D_x = 2.73$ Mg m^{-3}, Mo $K\alpha$, $\lambda = 0.71069$ Å, $\mu = 5.88$ mm^{-1}, $F(000) = 840$, room temperature, $R = 4.8\%$, $R_w = 5.7\%$ for 3639 independent reflections with $I > 4\sigma(I)$. The unit cell contains one $(V_{10}O_{28})^{6-}$ anion located on a symmetry center, two symmetry-related $[Er(H_2O)_8]^{3+}$ cations and nine interstitial water molecules, one with its O at a symmetry center. The structure forms layers of both decavanadate polyanions and rare-earth polyhedra (which do not share coordination O atoms), and layers of water molecules of hydration. These layers are parallel to (001) and are held together by hydrogen bonding.

Introduction. As part of a general study of the crystal chemistry of the rare-earth decavanadates (Rigotti, Punte, Rivero, Escobar & Baran, 1981, and references therein), we have solved the structure of $Er_2V_{10}O_{28}.25H_2O$, which is isostructural with Ln_2-$V_{10}O_{28}.25H_2O$ (Ln = Eu, Gd, Tb, Dy and Ho).

Experimental. Bright-orange crystalline plates of the hydrated rare-earth decavanadates grown and kindly supplied by Dr E. J. Baran and co-workers, Area de Quimica Inorgánica, UNLP, Argentina; syntheses have been described by Rigotti *et al.* (1981). Density measured pycnometrically. Crystal of irregular shape, $0.4 \times 0.4 \times 0.2$ mm. Enraf–Nonius CAD-4 diffractometer, graphite-monochromatized Mo $K\alpha$ radiation, ω/θ scan mode. Lattice parameters obtained from high 2θ values (17–30°) of 25 reflections. Scan width $(1 + 0.34\tan\theta)°$, aperture $(1.4 + 0.8\tan\theta)$ mm, maximum scan time 60 s, range explored 3.0 to 50.0° in 2θ. Three reflections (603, 654 and 7$\bar{3}$5) monitored every 100 reflections showed an overall σ (relative instability) of 0.02. 3639 unique reflections [$I > 4\sigma(I)$]

from a total of 7385, $R_{int} = 0.022$. Lp correction, absorption and extinction ignored. Heavy-atom method (*SHELX*, Sheldrick, 1976). All remaining (nonhydrogen) atoms from ΔF synthesis. Anisotropic blocked diagonal matrix and F magnitudes. f curves from Cromer & Mann (1968) for Er^{3+}, V^{5+} and O^- (for the decavanadate ion). Refinement with about 12 data per independent parameter, final $R = 0.048$, $R_w = 0.057$; $w = 16.6/[\sigma^2(F) + 0.0008F^2]$. $(\Delta/\sigma)_{max}$ 0.14; $(\Delta/\sigma)_{ave}$ 0.003. Max. and min. height in final $\Delta\rho$ map 2.99 and -4.94 e Å^{-3}.

Discussion. Final atomic coordinates are in Table 1.‡

The decavanadate polyanion $V_{10}O_{28}^{6-}$ is formed by a highly condensed system of VO_6 octahedra, shown in Fig. 1, as previously described for $K_2Zn_2V_{10}O_{28}$.-$16H_2O$ (Evans, 1966), $Ca_3V_{10}O_{28}.17H_2O$ (Swallow, Ahmed & Barnes, 1966), $Na_6V_{10}O_{28}.18H_2O$ (Durif, Averbuch-Pouchot & Guitel, 1980), $Y_2V_{10}O_{28}.24H_2O$, $La_2V_{10}O_{28}.20H_2O$ and $Nd_2V_{10}O_{28}.28H_2O$ (Saf'yanov, Kuz'min & Belov, 1979) and $[NHC_7H_9]_4[V_{10}H_2O_{28}]$ (Debaerdemaeker, Arrieta & Amigo, 1982).

Table 2 shows the interatomic distances and angles of the three types of VO_6 octahedra (Evans, 1966). Regarding the geometry of the decavanadate polyanion, two types of distortions can be discussed.

(a) Distortions of VO_6 octahedra, which do not significantly affect the intrinsic *mmm* orthorhombic symmetry of the polyanion. The severe distortions in the VO_6 octahedra – displacement of V_{III}-type atoms towards one edge of the octahedra and displacement of V_I and V_{II} towards one apex – are mainly due to internal Coulombic repulsion (Evans, 1966). These distortions can be interpreted on the grounds put forward by Baur (1970) and Brown & Shannon (1973). The empirical bond-strength–bond-length curves for

---

* Member of the Carrera del Investigador Cientifico, CIC, Provincia de Buenos Aires, Argentina.

† Member of the Carrera del Investigador Cientifico, CONICET, Argentina.

oxides proposed by the latter authors are very useful in accounting for bonding in highly distorted environments, since the concepts of ionic radius and coordination number are avoided. The correlation between distortion (mean-square relative deviation of bond length from the average) and average V–O bond length within each VO_6 octahedron in erbium decavanadate is similar to that given in Fig. 7 of Brown & Shannon (1973).

Table 1. *Fractional positional parameters and equivalent isotropic thermal parameters with e.s.d.'s in parentheses*

	x	y	z	$U_{eq}{}^*(Å^2)$
V(1)	0.0068 (1)	0.2162 (1)	0.6123 (1)	0.026
V(2)	0.9141 (1)	0.3547 (1)	0.3784 (1)	0.029
V(3)	0.9328 (1)	0.3532 (1)	0.7971 (1)	0.033
V(4)	0.8232 (1)	0.4913 (1)	0.5717 (1)	0.022
V(5)	0.2595 (1)	0.3697 (1)	0.6641 (1)	0.030
O(1)	0.9741 (5)	0.0622 (4)	0.6039 (4)	0.043
O(2)	0.9028 (5)	0.1946 (4)	0.7573 (4)	0.036
O(3)	0.1925 (5)	0.2064 (4)	0.6430 (4)	0.037
O(4)	0.8317 (4)	0.3137 (4)	0.5490 (3)	0.023
O(5)	0.0981 (4)	0.3222 (4)	0.4420 (3)	0.027
O(6)	0.0389 (4)	0.4393 (4)	0.6004 (3)	0.026
O(7)	0.8822 (5)	0.1971 (5)	0.3771 (4)	0.054
O(8)	0.7413 (4)	0.4400 (4)	0.3498 (4)	0.031
O(9)	0.0290 (5)	0.4491 (4)	0.2359 (4)	0.050
O(10)	0.8377 (5)	0.2982 (5)	0.9298 (4)	0.054
O(11)	0.1246 (5)	0.3147 (4)	0.8062 (4)	0.042
O(12)	0.7575 (5)	0.4263 (4)	0.7162 (4)	0.041
O(13)	0.3213 (4)	0.4464 (4)	0.4880 (3)	0.033
O(14)	0.4169 (5)	0.3259 (5)	0.6962 (4)	0.048
Er	0.4601 (1)	0.1303 (1)	0.2600 (1)	0.031
OW(15)	0.2860 (5)	0.0690 (5)	0.1678 (4)	0.055
OW(16)	0.5037 (5)	0.2824 (5)	0.3589 (4)	0.070
OW(17)	0.5935 (5)	0.0317 (5)	0.1234 (4)	0.056
OW(18)	0.6644 (6)	0.0397 (5)	0.3400 (4)	0.066
OW(19)	0.2477 (5)	0.1107 (5)	0.4011 (4)	0.058
OW(20)	0.3397 (6)	0.3412 (5)	0.1706 (4)	0.069
OW(21)	0.5978 (5)	0.1206 (5)	0.6415 (4)	0.060
OW(22)	0.6444 (6)	0.3056 (5)	0.1280 (5)	0.084
OW(23)	0.5358 (6)	0.2032 (5)	0.8962 (4)	0.067
OW(24)	0.1086 (6)	0.0015 (6)	0.9048 (5)	0.084
OW(25)	0.3283 (7)	0.4004 (6)	0.9399 (5)	0.088
OW(26)	0.0316 (8)	0.2083 (9)	0.1395 (7)	0.180
OW(27)†	0.0000	0.5000	0.0000	0.122

* Defined according to Hamilton (1959).
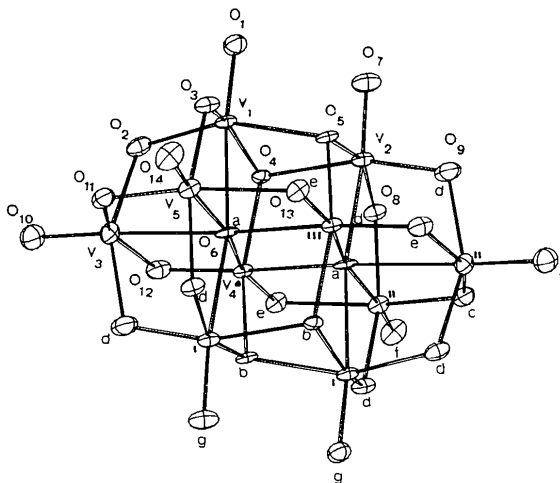† Site occupation factor 0.5.

Fig. 1. Arrangement of different V and O atom types in the decavanadate polyanion, according to Evans (1966).

(b) Distortions in the *mmm* symmetry arising from interactions with neighbouring atoms and groups. Table 3 shows the extreme and average values of the V–O distances and O–V–O angles for each type of V and O atom. The ranges spanned by each type are a measure of the distortion from *mmm* symmetry. These distortions are similar to those reported for $K_2Zn_2V_{10}O_{28}\cdot16H_2O$ (Evans, 1966) and correspond to deviations of no more than 0.04 Å and 2° from the distances and angles, respectively, reported by Evans. One of the more significant variations is observed in V(2)–O(8)/ V(2)–O(9) (V_I–Od type) where a stronger hydrogen bond to O(8) lengthens V(2)–O(8) by 0.031 Å (Table 2) with respect to V(2)–O(9), where O(8) and O(9) are related by the pseudomirror plane. This fact is supported by an O(8)$\cdots OW$(16) distance of 2.662 Å compared to O(9)$\cdots OW$(27) = 2.924 Å. Similar variations in interbond distances for V_{II}–Od, V_{III}–Ob and V_I–Ob cannot be explained without the knowledge of the H positions due to the possibility of bifurcated and trifurcated hydrogen bonds (*cf.* Brink, 1971; Knop, Westerhaus & Falk, 1980, and references therein).

Table 2. *Interatomic distances (Å) and interbond angles (°) in the VO_6 and ErO_8 polyhedra (e.s.d.'s in parentheses)*

V_I V(1)	Og O(1)	Od' O(2)	Od O(3)	Ob' O(4)	Ob O(5)	Oa O(6)
Og O(1)	1.617 (5)	2.696 (7)	2.710 (7)	2.752 (6)	2.737 (5)	3.808 (7)
Od' O(2)	103.2 (2)	1.819 (4)	2.719 (6)	2.702 (6)	3.761 (7)	2.645 (5)
Od O(3)	103.9 (2)	96.7 (2)	1.821 (5)	3.771 (6)	2.722 (6)	2.654 (6)
Ob' O(4)	97.2 (2)	88.9 (2)	156.2 (2)	2.032 (4)	2.511 (5)	2.607 (6)
Ob O(5)	96.9 (2)	156.6 (2)	90.0 (2)	76.6 (2)	2.022 (4)	2.632 (7)
Oa O(6)	171.6 (2)	81.7 (2)	82.0 (2)	75.9 (2)	77.0 (2)	2.200 (5)

V_I V(2)	Ob' O(4)	Ob O(5)	Oa O(6')	Og O(7)	Od' O(8)	Od O(9)
Ob' O(4)	2.023 (4)	2.511 (5)	2.613 (7)	2.780 (7)	2.695 (6)	3.740 (7)
Ob O(5)	77.3 (2)	1.998 (4)	2.618 (7)	2.769 (7)	3.746 (6)	2.678 (6)
Oa O(6')	75.6 (2)	76.3 (2)	2.230 (5)	3.838 (7)	2.660 (6)	2.657 (7)
Og O(7)	99.1 (2)	99.6 (2)	173.9 (2)	1.613 (5)	2.684 (6)	2.675 (5)
Od' O(8)	88.5 (2)	155.6 (2)	81.1 (2)	102.1 (2)	1.833 (4)	2.706 (6)
Od O(9)	155.8 (2)	89.5 (2)	81.7 (2)	103.0 (2)	96.2 (2)	1.802 (4)

V_{II} V(3)	Od O(2)	Oa O(6)	Od O(9')	Of O(10)	Oc O(11)	Oe O(12)
Od O(2)	1.868 (5)	2.645 (5)	3.660 (6)	2.700 (8)	2.666 (7)	2.603 (6)
Oa O(6)	77.7 (2)	2.312 (5)	2.657 (6)	3.920 (7)	2.743 (6)	2.658 (5)
Od O(9')	153.8 (2)	77.7 (2)	1.889 (4)	2.727 (7)	2.681 (7)	2.622 (6)
Of O(10)	101.3 (2)	172.4 (2)	101.9 (2)	1.617 (4)	2.730 (6)	2.808 (7)
Oc O(11)	92.7 (2)	82.4 (2)	92.8 (2)	105.2 (2)	1.815 (5)	3.813 (6)
Oe O(12)	82.3 (2)	74.3 (1)	82.6 (2)	98.1 (2)	156.7 (2)	2.079 (5)

V_{III} V(4)	Ob O(4)	Ob' O(5')	Oa O(6)	Oa' O(6')	Oe O(12)	Oe' O(13')
Ob O(4)	1.898 (4)	3.752 (6)	2.607 (5)	2.613 (6)	2.706 (7)	2.709 (5)
Ob' O(5')	155.4 (2)	1.942 (5)	2.618 (5)	2.632 (7)	2.720 (6)	2.678 (7)
Oa O(6)	80.9 (2)	80.3 (2)	2.113 (4)	2.650 (8)	2.658 (5)	3.750 (7)
Oa' O(6')	80.3 (2)	80.1 (2)	77.0 (2)	2.143 (5)	3.792 (6)	2.661 (5)
Oe O(12)	98.1 (2)	97.1 (2)	88.2 (2)	165.2 (2)	1.681 (4)	2.697 (7)
Oe' O(13')	98.6 (2)	95.3 (2)	164.5 (2)	87.6 (2)	107.2 (2)	1.671 (4)

V_{II} V(5)	Od O(3)	Oa O(6)	Od O(8')	Oc O(11)	Oe O(13)	Of O(14)
Od O(3)	1.878 (5)	2.654 (6)	3.632 (6)	2.628 (7)	2.586 (5)	2.713 (7)
Oa O(6)	77.0 (2)	2.345 (4)	2.660 (7)	2.743 (6)	2.661 (5)	3.939 (7)
Od O(8')	154.3 (2)	77.8 (2)	1.847 (4)	2.639 (6)	2.650 (5)	2.688 (7)
Oc O(11)	89.6 (2)	80.7 (2)	91.1 (2)	1.851 (4)	3.793 (6)	2.724 (6)
Oe O(13)	82.6 (2)	74.5 (2)	86.0 (2)	155.0 (2)	2.034 (4)	2.810 (6)
Of O(14)	102.4 (2)	175.2 (2)	102.4 (2)	104.1 (2)	100.7 (2)	1.597 (5)

Table 2 *(cont.)*

Er	O(15)	O(16)	O(17)	O(18)	O(19)	O(20)	O(21')	O(22)
O(15)	2·375 (6)	4·512 (6)	2·800 (7)	4·438 (7)	3·085 (8)	2·786 (8)	2·890 (7)	3·905 (8)
O(16)	143·2 (2)	2·380 (6)	4·496 (7)	2·881 (7)	2·762 (7)	2·975 (8)	4·149 (7)	2·864 (8)
O(17)	71·8 (2)	140·2 (2)	2·402 (5)	2·989 (8)	4·499 (8)	3·991 (7)	2·971 (7)	2·808 (8)
O(18)	140·5 (2)	75·2 (2)	78·1 (2)	2·341 (5)	3·841 (6)	4·524 (7)	2·824 (8)	3·065 (6)
O(19)	82·6 (2)	72·3 (2)	146·2 (2)	111·7 (2)	2·300 (4)	2·951 (5)	2·854 (6)	4·347 (7)
O(20)	71·5 (2)	77·1 (2)	112·7 (2)	145·8 (2)	77·9 (2)	2·391 (5)	4·466 (7)	2·772 (8)
O(21')	75·0 (2)	121·7 (2)	77·0 (2)	73·6 (2)	75·3 (2)	139·3 (2)	2·371 (6)	4·482 (8)
O(22)	111·9 (2)	74·8 (2)	72·7 (2)	81·8 (2)	139·2 (2)	71·8 (2)	144·2 (2)	2·338 (5)

Table 3. *Average bond distances (Å) and angles (°) in the decavanadate ion*

Numbers of averaged values are given in parentheses.

	Average	Range
V_I–Og	1·62 (2)	1·613–1·617
V_I–Oa	2·22 (2)	2·200–2·230
V_I–Ob	2·02 (4)	1·998–2·032
V_I–Od	1·82 (4)	1·802–1·833
V_{II}–Of	1·61 (2)	1·597–1·617
V_{II}–Oa	2·33 (2)	2·312–2·345
V_{II}–Oc	1·83 (2)	1·815–1·851
V_{II}–Od	1·87 (4)	1·847–1·889
V_{II}–Oe	2·06 (2)	2·034–2·079
V_{III}–Oe	1·68 (2)	1·671–1·681
V_{III}–Oa	2·13 (2)	2·113–2·143
V_{III}–Ob	1·92 (2)	1·898–1·942
Og–V_I–Ob	98 (4)	96·9– 99·6
Og–V_I–Od	103 (4)	102·1–103·9
Oa–V_I–Ob	76 (4)	75·6– 77·0
Oa–V_I–Od	82 (4)	81·1– 82·0
Ob–V_I–Ob'	77 (2)	76·6– 77·3
Od–V_I–Od'	96 (2)	96·2– 96·7
Ob–V_I–Od	89 (4)	88·5– 90·0
Ob–V_I–Od'	156 (4)	155·6–156·6
Oa–V_I–Og	173 (2)	171·6–173·9
Of–V_{II}–Oe	99 (2)	98·1–100·7
Oa–V_{II}–Oe	74 (2)	74·3– 74·5
Of–V_{II}–Oc	105 (2)	104·1–105·2
Of–V_{II}–Od	102 (4)	101·3–102·4
Oa–V_{II}–Oc	82 (2)	80·7– 82·4
Oa–V_{II}–Od	78 (4)	77·0– 77·8
Oc–V_{II}–Od	92 (4)	89·6– 92·8
Od–V_{II}–Oe	83 (4)	82·3– 86·0
Oa–V_{II}–Of	174 (2)	172·4–175·2
Oc–V_{II}–Oe	156 (2)	155·0–156·7
Od–V_{II}–Od	154 (2)	153·8–154·3
Oe–V_{III}–Oe'	107 (1)	107·2
Oa–V_{III}–Oa'	77 (1)	77·0
Oa–V_{III}–Oe	88 (2)	87·6– 88·2
Oa–V_{III}–Ob	80 (4)	80·1– 80·9
Ob–V_{III}–Oe	97 (4)	95·3– 98·6
Ob–V_{III}–Ob'	155 (1)	155·4
Oa–V_{III}–Oe'	165 (2)	164·5–165·2

Fig. 2. Stereoscopic view of the structure down **a*** with **b*** horizontal.

However, hydrogen bonding alone cannot explain the observed differences in interbond distances for the cases in which these forces are not operating, that is for V_{III}–Oe type (very loosely hydrogen bonded) and for V_{III}–Oa type (Oa type are not sterically accessible to a water molecule). Thus, at present there is no satisfactory explanation for the deviations from *mmm* symmetry.

The three ideal mean planes corresponding to the symmetry planes were calculated with a modified version of *NRC*22 (Ahmed & Pippy, 1966), which includes the calculation of the standard deviation of the dihedral angles according to Ito (1981).* Dihedral angles between these planes are 89·86 (1), 90·30 (1)
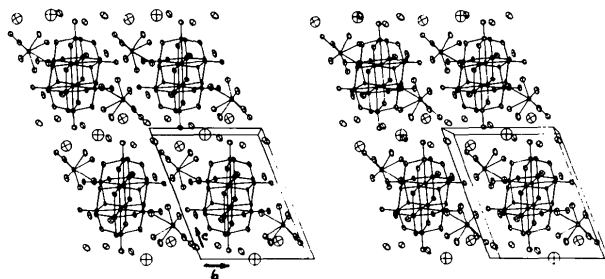
* See deposition footnote.

and 90·11 (1)°. χ^2 values [$\chi^2 = \Sigma(\Delta/\sigma)^2$] for the three mean planes (77·7, 165·0 and 4·7, respectively), indicate significant deviation from coplanarity in the two former cases. The χ^2 value for the third plane would indicate true *m* symmetry; however, the analysis of the distances to this plane of the assumed mirror-symmetry-related pairs of atoms indicates significant deviations from *m* symmetry (*i.e.* the standard deviation is 0·02 against 0·008 Å expected from experimental errors).

A stereoscopic projection of the unit cell down **a*** is shown in Fig. 2. It can be seen that the structure is formed by layers of decavanadate ions and hydrated Er^{3+} ions parallel to (001), which are linked together by ionic forces and hydrogen bonds formed by interstitial and coordination water with O atoms in $V_{10}O_{28}^{6-}$. Intercalated layers of interstitial water molecules parallel to (001) are also clearly seen in the projection. Decavanadate groups and rare-earth polyhedra do not share coordination O atoms. The coordination polyhedron of Er^{3+} ions is a distorted square antiprism (Wells, 1975), with the Er—O and O—O distances given in Table 2.

In the last stages of refinement, a Fourier synthesis revealed the presence of an unexpected water molecule at a symmetry center. There are several reported structures in which the water molecules occupy site symmetries other than C_{2v} or its subgroups (*cf.* Guggenberger & Sleight, 1969; Jensen, 1968; Pierce-Butler, 1982). Librational rather than orientational disorder may be invoked to explain the existence of this 'centrosymmetric' water molecule, since it does not interact appreciably with neighboring groups, the

distances O—acceptor and the angles acceptor—O—acceptor not being favorable for the formation of strong hydrogen bonds.

In a previous paper (Rigotti *et al.*, 1981) we reported the crystalline structure for the complete series of rare-earth decavanadates and wrongly described erbium decavanadate (Group III) as a 24-hydrate. It now seems reasonable to assume that structural differences between Groups III and IV are mainly due to the occupancy of a symmetry center by an interstitial water molecule, rather than by changes in the Ln^{3+} ionic radii, or any other inherent feature of the Ln^{3+} ions.

References

AHMED, F. R. & PIPPY, M. E. (1966). *NRC* Crystallographic Programs for the IBM 360 system. *NRC*22, revised June 1970. Division of Pure Physics, National Research Council of Canada, Ottawa.

BAUR, W. H. (1970). *Trans. Am. Crystallogr. Assoc.* **6**, 129–155.
BRINK, G. (1971). *Spectrochim. Acta Part A*, **28**, 1151–1155.
BROWN, I. D. & SHANNON, R. D. (1973). *Acta Cryst.* A**29**, 266–282.
CROMER, D. T. & MANN, J. B. (1968). *Acta Cryst.* A**24**, 321–324.
DEBAERDEMAEKER, T., ARRIETA, J. M. & AMIGO, J. M. (1982). *Acta Cryst.* B**38**, 2465–2468.
DURIF, P. A., AVERBUCH-POUCHOT, M. T. & GUITEL, J. C. (1980). *Acta Cryst.* B**36**, 680–682.
EVANS, H. T. (1966). *Inorg. Chem.* **5**, 967–977.
GUGGENBERGER, L. J. & SLEIGHT, A. W. (1969). *Inorg. Chem.* **8**, 2041–2046.
HAMILTON, W. C. (1959). *Acta Cryst.* **12**, 609–610.
ITO, T. (1981). *Acta Cryst.* A**37**, 621–624.
JENSEN, S. J. (1968). *Acta Chem. Scand.* **22**, 647–652.
KNOP, O., WESTERHAUS, W. J. & FALK, M. (1980). *Can. J. Chem.* **58**, 867–874.
PIERCE-BUTLER, M. A. (1982). *Acta Cryst.* B**38**, 3097–3100.
RIGOTTI, G., PUNTE, G., RIVERO, B. E., ESCOBAR, M. E. & BARAN, E. J. (1981). *J. Inorg. Nucl. Chem.* **43**, 2811–2814.
SAF'YANOV, YU. N., KUZ'MIN, E. A. & BELOV, N. V. (1979). *Kristallografiya*, **24**, 767–771.
SHELDRICK, G. M. (1976). *SHELX*76. Program for crystal structure determination. Univ. of Cambridge, England.
SWALLOW, A. G., AHMED, F. R. & BARNES, W. H. (1966). *Acta Cryst.* **21**, 397–405.
WELLS, A. F. (1975). *Structural Inorganic Chemistry*, 4th ed., p. 64. Oxford: Clarendon Press.

Structure of Monoclinic Rubidium Dideuteriumphosphate, RbD₂PO₄, in the Intermediate Phase

BY T. HAGIWARA, K. ITOH AND E. NAKAMURA

Faculty of Science, Hiroshima University, Hiroshima 730, Japan

AND M. KOMUKAE AND Y. MAKITA

Department of Applied Physics, Faculty of Science, Science University of Tokyo, Kagurazaka, Shinjuku-ku, Tokyo 162, Japan

Abstract. $M_r = 184.44$, monoclinic, $P2_1/c$, $a = 7.683$ (1), $b = 6.170$ (1), $c = 9.560$ (1) Å, $\beta = 109.10$ (1)°, $V = 428.2$ Å³, $Z = 4$, $D_x = 2.861$ g cm⁻³, $\lambda(\text{Cu } K\alpha) = 1.54178$ Å, $\mu(\text{Cu } K\alpha) = 202.16$ cm⁻¹, $F(000) = 344$, $T = 332$ K, $R = 0.040$ for 500 unique reflections. The intermediate phase has a superstructure of the basic CsH_2PO_4 type. The shape of the PO_4 tetrahedron is rather regular. Two kinds of H atoms display extremely large thermal amplitudes of about 0.5 Å. PO_4 tetrahedra are connected by these H atoms to form a zigzag chain running along **b**.

Introduction. Monoclinic RbD_2PO_4 undergoes successive phase transitions at 377 and 317 K (Sumita,

Osaka & Makita, 1981). It is known that the low-temperature phase is ferrielectric and the intermediate and the high-temperature phases are paraelectric (Osaka, Sumita & Makita, 1983). The crystal structure of the low-temperature phase was determined at room temperature by Makita, Sumita, Osaka & Suzuki (1981). However, the structures of the other phases have not yet been determined. It is necessary to investigate the structures of these higher-temperature phases in order to clarify the mechanism of the successive phase transitions from the structural point of view. We now report the crystal structure of the intermediate phase, as part of a continuing study of the mechanism of the successive phase transitions.